processes

MDPI

Article

Laser-Induced Ignition and Combustion of Individual Aluminum Particles Below 10 μm by Microscopic High-Speed Cinematography

Fengting Hou [1], Shengji Li [2,*], Yue Wang [1] and Xuefeng Huang [1,*]

[1] Institute of Energy, Department of Physics, Hangzhou Dianzi University, Hangzhou 310018, China; hft_energy@126.com (F.H.); coldfire1@163.com (Y.W.)
[2] College of Materials and Environmental Engineering, Hangzhou Dianzi University, Hangzhou 310018, China
* Correspondence: shengjili@hdu.edu.cn (S.L.); xuefenghuang@hdu.edu.cn (X.H.); Tel.: +86-571-8687-8677 (X.H.)

Received: 4 February 2020; Accepted: 24 February 2020; Published: 28 February 2020

Abstract: Metal aluminum has been widely used as an ingredient in propellant, gunpowder and thermite, but there is less understanding of the combustion mechanism of aluminum particles from submicron to several microns in diameter. This paper proposes to experimentally investigate the ignition and combustion characteristics of individual aluminum particles below 10 μm. A specific in situ diagnostic experimental apparatus was first designed for directly observing the ignition and combustion behaviors of individual aluminum particles, with a submicrometer spatial resolution and a temporal resolution of tens of microseconds. Direct observation through microscopic high-speed cinematography demonstrated that, when heated by a continuous laser, individual aluminum particles thermally expanded, followed by shell rupture; the molten aluminum core overflowed and evaporated, leading to ignition and combustion. Further results showed that, when the laser power densities were gradually increased (5.88, 7.56 and 8.81 × 10^5 W/cm^2), the durations of thermal expansion, melting and evaporation were shortened. The required time for the aluminum particles to expand to 150% of their initial diameter was shortened (34 s, 0.34 s and 0.0125 s, respectively). This study will be beneficial to further extend the investigation of other individual metal particles and reveal their combustion mechanism by direct observation.

Keywords: individual aluminum; submicron particle; microscopic high-speed cinematography; laser ignition; combustion mechanism

1. Introduction

Aluminum has been widely used as an additional metal additive in solid rocket propellants to improve their combustion performance. However, the ignition and combustion characteristics of aluminum vary significantly with different sizes and operating conditions. Friedman et al. [1,2] reported the ignition and subsequent combustion of aluminum particles ranging from 15 to 67 μm and showed how the ambient gas temperature and oxygen content influenced the combustion performance of aluminum. Roberts et al. [3] reported that aluminum particles with an average diameter of 20 μm were ignited in oxygen using the reflected shock wave in a single-pulse shock tube. Maček et al. [4] observed the ignition and combustion characteristics of individual aluminum particles of 32–49 μm diameter in a gas environment of known composition and temperature. Davis [5] used high-speed cinematography to observe the burning process of aluminum particles with initial diameters ranging from 53 to 103 μm. These results illustrate that, for micron-sized aluminum particles, the ignition temperature occurs upon melting of the oxide shell at ~2300 K, and the burning time of 10~100 μm

aluminum follows an exponential relationship to the diameter (t-$D^{1.2–1.5}$). However, for aluminum particles ranging from submicron to several microns in diameter, their ignition and combustion characteristics have remained veiled.

In the past few decades, many ignition patterns have been attempted to unveil the combustion characteristics of aluminum particles, mainly including laser beam [6], electric heating wire [7,8], flat flame burner [1,2], shock tube [9,10], stroboscopic lamp [11], hot air [12], etc. Legrand et al. [13] reported that the surface exothermic process plays a leading role in aluminum combustion by a laser ignition system. Zhu et al. [7] used a high frequency induction heating wire to ignite a solid aluminum cylinder placed in the stagnation region of the oxygen/nitrogen mixture stream and recorded the ignition temperature. Friedman et al. [1,2] utilized two methods to obtain experimental data; one was to inject aluminum particles into the hot gas stream produced by the flat flame burner, and the other was to burn the particles in the combustion products of the ammonium perchlorate flame. Bazyn et al. [9] used the shock tube to study the flame radiation intensity and peak burning temperature of the aluminum. Ohkura et al. [11] ignited nano-aluminum powder for the first time with a strobe light and provided direct experimental evidence to show that the oxidation followed a melting dispersion mechanism. Derevyaga et al. [12] investigated the combustion of aluminum in an inductor and in a stream of hot gas blown through a tubular electric furnace. Among these ignition methods, laser ignition has some advantages over others, including: (i) the ignition source can be positioned a considerable distance from the point of ignition, thus eliminating distortions of intrusive sources; (ii) integration with the microimaging system simplifies the system complexity; and (iii) the power of the flux levels can be utilized and highly focused to a point, sheet or core, thus offering the ability to direct energy input to specific modes or configurations of the ignition.

It is noted that, for the experimental apparatus reported, when directly observing the ignition and combustion of individual aluminum particles, the smallest particle size was tens of microns. Submicron aluminum particles were usually ignited in the form of particle aggregates. This triggered our motivation to propose a new experimental method by combining laser ignition and microscopic high-speed cinematography to obtain the ignition and combustion characteristics of individual aluminum particles with diameters from submicron to several microns and to make a comparison to the ignition and combustion models proposed by many scholars [14–17]. In this study, firstly, an experimental apparatus was designed and built. The laser was accurately focused on individual aluminum particles for heating. The high-speed camera with microscopy was used to record the ignition and combustion processes. Secondly, digital microscopic images by calibration were utilized to identify the key ignition and combustion processes and to obtain parameters such as ignition delay and flame propagation speed. Finally, the effect of laser power density on the ignition and combustion characteristics of individual aluminum particles was conducted for exploring the ignition and combustion mechanism of aluminum.

2. Materials and Methods

The aluminum powder was purchased from Changsha Tianjiu Corporation, Changsha, China. Its purity reaches 99.8%, but it contains impurities of Fe, Si, Cu, O, etc. The schematic of the experimental apparatus is shown in Figure 1. A continuous near infrared laser set at 1064 nm and TEM_{00} (New Industries Optoelectronics Tech. Co. Ltd., Changchun, China) was used. The laser power was varied from 0 to 600 mW by tuning the modulated current magnitude. The laser beam was split into two beams by a splitter (7:3). The dominant beam was again shaped by a beam expander (3×), dichroic mirror and objective lens to focus on an individual aluminum particle and ignite it. The other beam directly reached the power meter (S350C, Thorlabs Inc., Newton, NJ, USA) to measure the ignition power. To obtain high resolution images of the aluminum particles, the objective with a high numerical aperture (NA) was required. Therefore, the objective was a key part and was used to highly focus the laser beam and simultaneously image the aluminum particles. In this apparatus, an objective with a NA of 0.65 and 40× (Olympus, Tokyo, Japan) was selected; its resolution can reach ~0.7 μm.

The high-speed camera (Phantom Micro M310, Vision Research Inc., Wayne, NJ, USA) was used to record the images during the ignition and combustion of aluminum. For clear imaging, an illuminator (Constellation 120E, Integrated Design Tools Inc., Pasadena, CA, USA) and condenser needed to be supplied. To avoid the interference of the laser beam on the imaging, a notch filter was installed in front of the high-speed camera. Comprehensively considering the spatial and temporal resolutions of imaging during the ignition and combustion of individual aluminum particles, the maximum recording frame of the high-speed camera could reach 11,000 fps.

The combustor was installed on a 3-axis translation platform and opened in air. Aluminum particles were placed at the bottom wall of the combustor. Therefore, the aluminum particles settled in air at normal pressure and room temperature. In this study, tens of individual aluminum particles were selected to conduct the ignition and combustion experiments. The power density ranged from 5.88 to 9.49×10^5 W/cm^2. If the power densities were too low, the aluminum particles would not ignite. Under each operating condition, six runs of experiments were conducted.

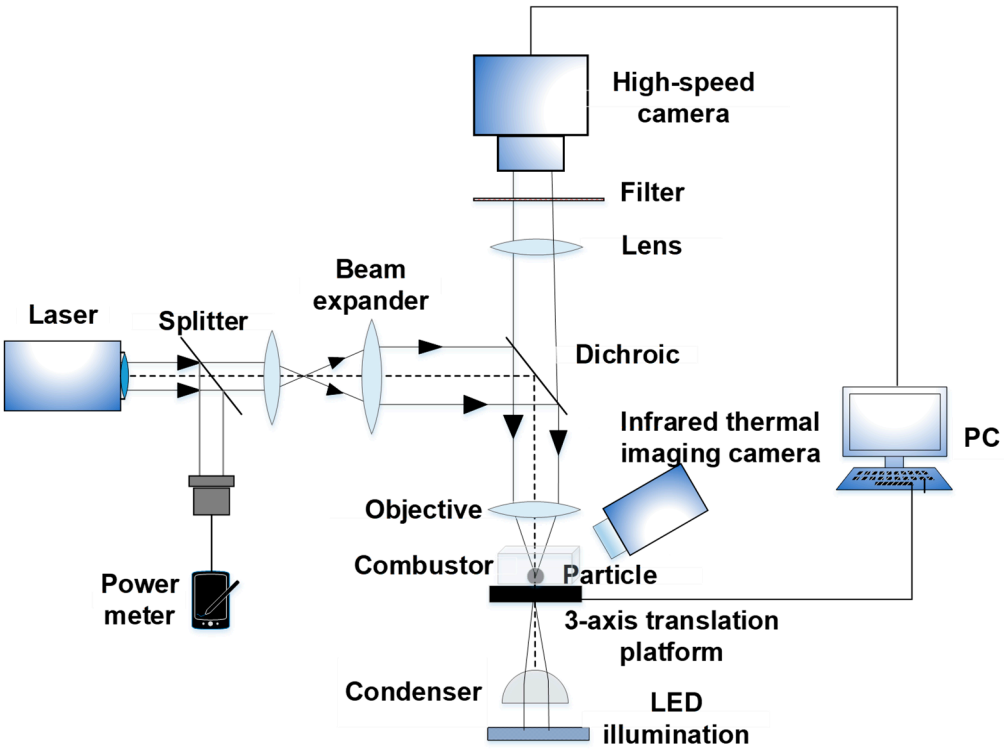

Figure 1. Schematic of experimental apparatus.

Since the aluminum particles were directly lying at the bottom wall of the combustor, the heat loss of the combustor wall possibly had an effect on the ignition. To evaluate the heat loss, an infrared thermal imaging camera was used to measure the temperature rise of the combustor wall as the aluminum particles were heated by the laser. The recording frame rate of the infrared thermal imaging camera was set to 200 fps. Figure 2 shows the temperature rises of an individual particle and the combustor bottom wall below the particle heated by the laser at a power density of 8.85×10^5 W/cm^2. As shown, the particle and the wall had the same temperature change trend; however, the temperature difference gradually increased. Therefore, the heat loss of the combustor wall could not be ignored due to the heat conduction from the aluminum to the wall during heating.

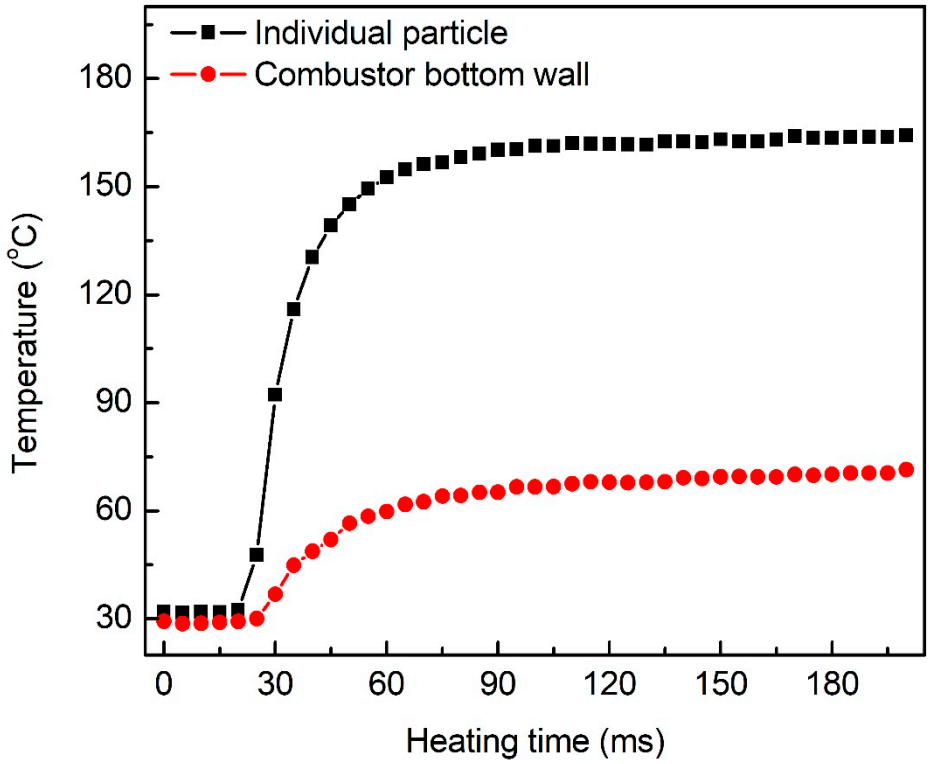

Figure 2. The temperature evolutions of an individual particle and the combustor bottom wall below the particle heated by the laser at a power density of 8.85×10^5 W/cm^2.

3. Results and Discussion

Using microscopic high-speed cinematography, the observed ignition and combustion evolution of an individual aluminum particle settled in air and ignited by laser is shown in Figure 3. The whole process can be seen in Supplementary Materials, Video S1. During ignition and combustion, the laser continuously heated the particle until extinction. The aluminum particle looked black and had a high circularity (Figure 3a). Its diameter was 6.82 μm. In this case, the laser power density was 5.88×10^5 W/cm^2. On heating, the aluminum particle thermally expanded, and the particle diameter significantly increased. In Figure 3, the above right part of the particle was slightly flat, indicating that the thermal expansion of aluminum was heterogeneous. As the aluminum particle was continuously heated by the laser, the above right part of the particle bulged, and the particle shape returned to spherical. This suggests that the aluminum particle started to melt (Figure 3c). During the period of Figure 3d,e, the particle edge became unsmooth. It might be inferred that cracks occurred and resulted in a rupture of the alumina thin film. During the period for Figure 3f–g, significant deformation of the above right part of the particle was observed, suggesting that the heated aluminum core melted and overflowed from the ruptured Al_2O_3 shell. At the moment of Figure 3h, much more liquid aluminum overflowed, and the particle shape became irregular. In Figure 3i–k, the particle edge suddenly enlarged, indicating that the aluminum particle almost completely melted and evaporated. Figure 3l–p show that a weak flare stood on the surface of the aluminum particle. It can be inferred that the heat absorbed by the aluminum particle was close to the ignition energy threshold; thus, the individual aluminum particle was heterogeneously ignited. After that, the aluminum particle extinguished quickly. In order to observe the change in particle shape more clearly, the pictures obtained by digital imaging treatment are shown in Figure 4. The entire deformation process of the individual aluminum particle can be clearly identified. Owing to the appearance of the flame, the particle profile was covered by the flame, and the particle images looked irregular like a crescent (Figure 4l–n).

Figures 5 and 6 demonstrate two other cases as the laser power density was enhanced to 7.56 and 8.81×10^5 W/cm^2. The diameters of these aluminum particles were 6.67 and 6.25 μm, respectively.

As shown, the two individual aluminum particles had deformations similar to that in Figure 4 during ignition and combustion.

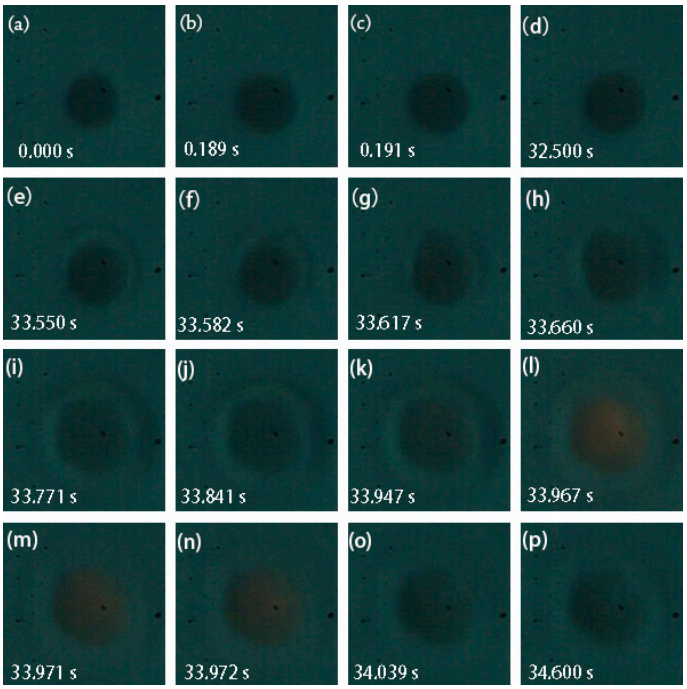

Figure 3. Representative snapshots of laser-induced ignition and combustion processes of an individual aluminum particle. The diameter was 6.82 μm. The laser power density was 5.88×10^5 W/cm^2. (Images acquired from Supplementary Materials, Video S1; recording frame: 11,000 fps; exposure time: 90.9 μs).

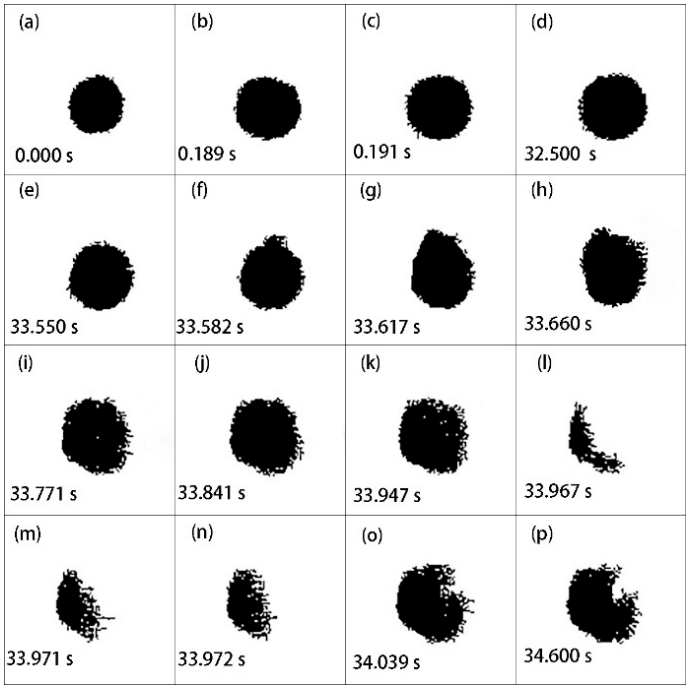

Figure 4. Representative pictures of laser-induced ignition and combustion processes of an individual aluminum particle using digital imaging treatment. The initial diameter was 6.82 μm. The laser power density was 5.88×10^5 W/cm^2.

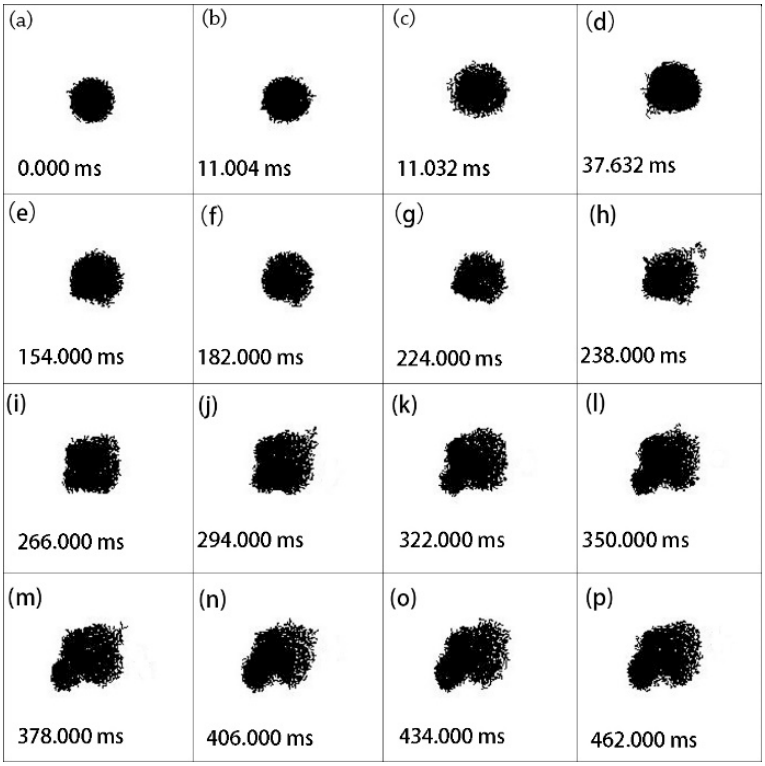

Figure 5. Representative pictures of laser-induced ignition and combustion processes of an individual aluminum particle using digital imaging treatment. The initial diameter was 6.67 μm. The laser power density was 7.56×10^5 W/cm^2.

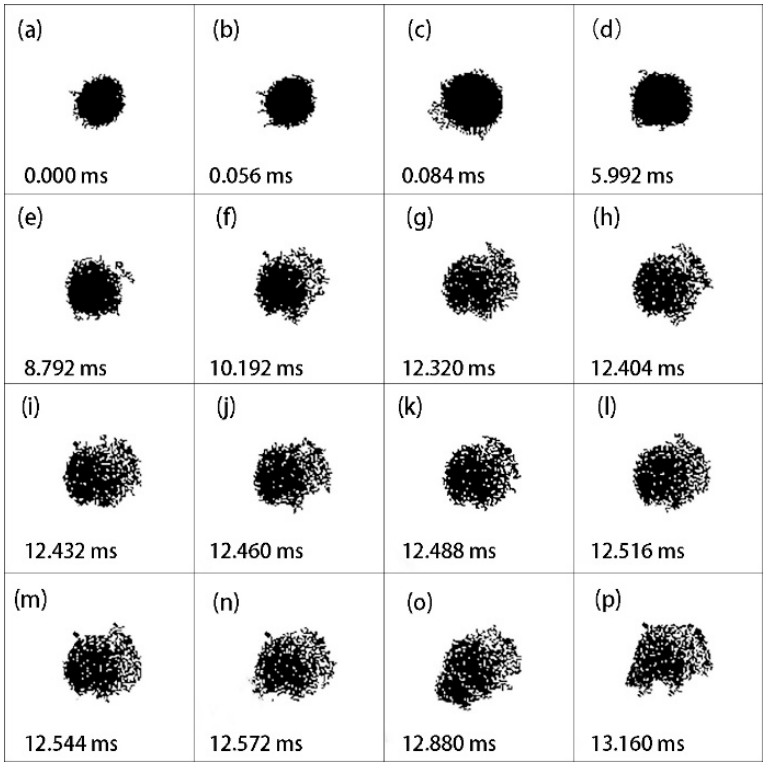

Figure 6. Representative pictures of laser-induced ignition and combustion processes of an individual aluminum particle using digital imaging treatment. The initial diameter was 6.25 μm. The laser power density was 8.81×10^5 W/cm^2.

From Figure 5, it can be clearly seen that the original shape of the aluminum particle was spherical with good circularity, and the particle expanded uniformly at 11.032 ms (Figure 5c). Subsequently, the lower left part of the particle gradually deformed (Figure 5d). As it evolved, the lower left part gradually became larger (Figure 5e–p), which resulted from the molten aluminum core spreading outward from the cracks of the alumina shell. In this case, the phenomenon provided direct evidence that the oxidation process of micron-sized aluminum was anisotropic and that the molten aluminum core erupted outward. For nanoscale aluminum, the phenomenon of anisotropic oxidation has been testified by Koga [18]. However, for aluminum below 10 μm, this is the first observation.

According to the changes of particle size, shape and phase state shown in Figures 4–6, the aluminum particles underwent several stages after being heated by the laser: thermal expansion, alumina shell rupture, molten aluminum core overflow, shell melt and aluminum evaporation, ignition and combustion. Direct observation in Figure 7 shows the evolution of the aluminum particle diameter and circularity. It is apparent that the evolution included three stages: (i) thermal expansion, (ii) melting and (iii) evaporation. This was in agreement with our previous result that the three distinctive stages represented heating, melting and evaporation until ignition [6]. Yang et al. [19] and Ermakov et al. [20] have reported the three-stage phenomenon for micron-sized aluminum during ignition. Trunov et al. [21] developed a simplified ignition model and assumed that ignition occurs when the particle temperature exceeds the alumina melting point. Rai et al. [22] demonstrated that prior to the melting of aluminum, slow oxidation occurs due to the diffusion of oxygen through the aluminum oxide shell.

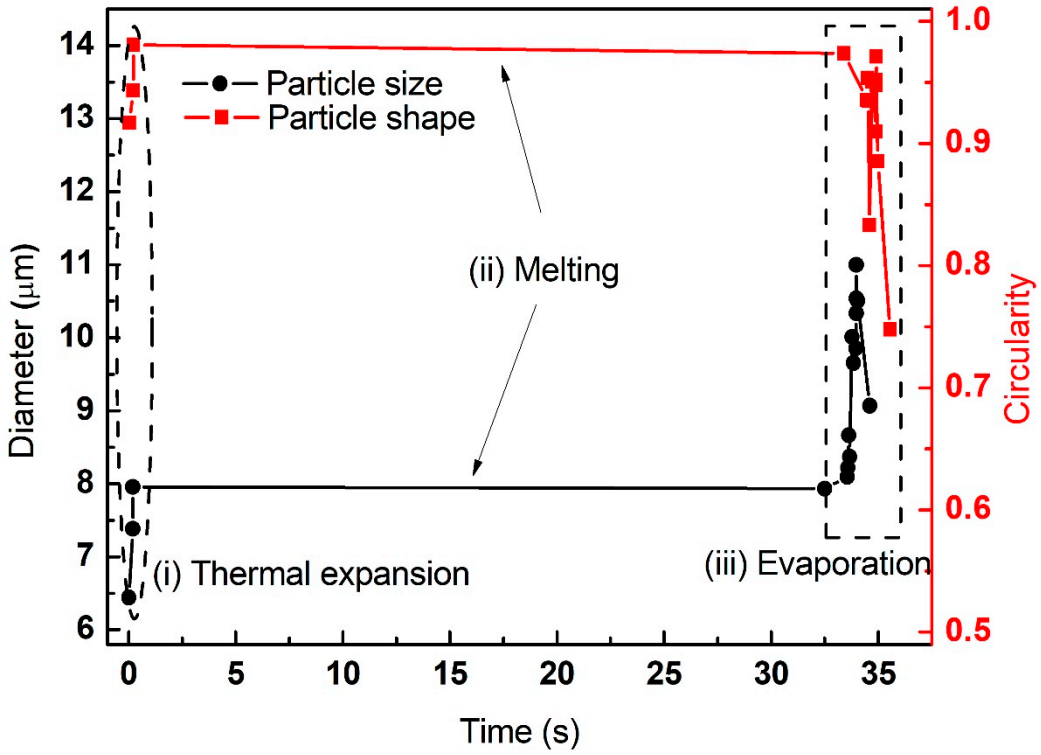

Figure 7. The variation of particle diameter and circularity of individual aluminum particles (initial diameter of 6.82 μm, laser power density of 5.88×10^5 W/cm^2).

The variation of particle diameter and circularity of the individual aluminum particles at elevated laser power densities are summarized in Figures 7–9. The initial diameters of three individual aluminum particles were approximately equivalent to 6.82 μm, 6.67 μm and 6.25 μm, respectively. The laser power densities were gradually increased (5.88×10^5 W/cm^2, 7.56×10^5 W/cm^2 and 8.81×10^5 W/cm^2, respectively). For micron-sized aluminum, the three stages of thermal expansion, melting and

evaporation were clearly identified. Moreover, the duration of each stage shortened. For example, the heating time required for the equivalent diameter of particles to expand to 150% of their initial diameter was 34 s, 0.34 s and 0.0125 s, respectively. The laser power densities had a significant effect on the ignition and combustion of individual aluminum particles.

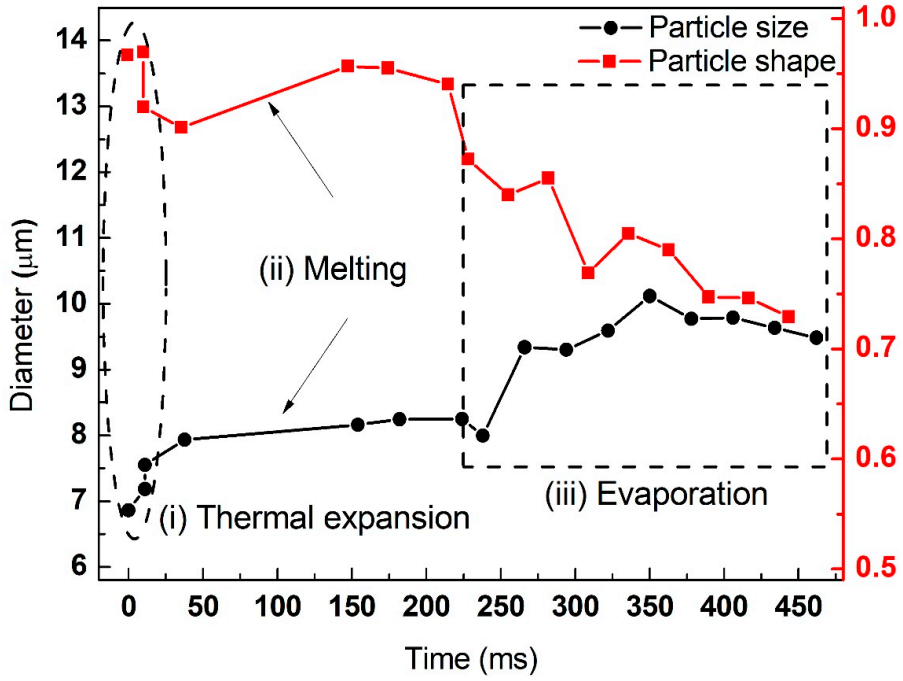

Figure 8. The variation of particle diameter and circularity of individual aluminum particles (initial diameter of 6.67 μm, laser power density of 7.56×10^5 W/cm^2).

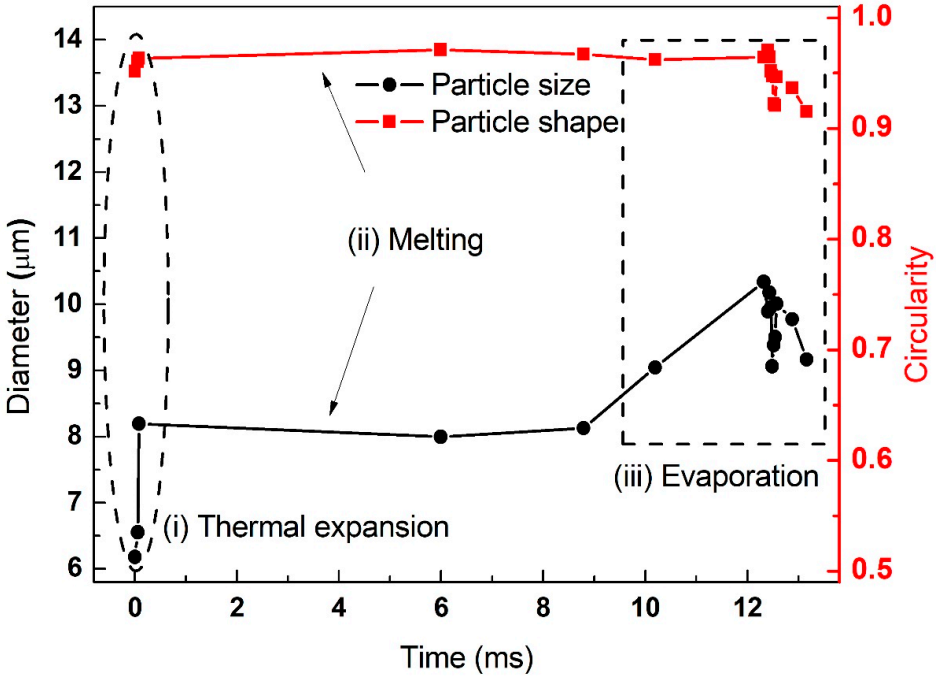

Figure 9. The variation of particle diameter and circularity of individual aluminum particles (initial diameter of 6.25 μm, laser power density of 8.81×10^5 W/cm^2).

According to the diffusion oxidation mechanism, the oxidation process of aluminum particles is mainly affected by the internal Al cations and the external O migration rates [23]. The size distribution of the particles is a crucial factor affecting the oxidation rate. As the particle size decreases, the oxidation rate accelerates. However, according to the melt dispersion mechanism, when the heating rate is high enough, a phase change occurs inside the aluminum particles. It causes the internal stress to exceed the strength limit of the oxide layer, and the molten aluminum sprays out at a high speed through the oxide layer. The oxidation of sprayed small particles is no longer limited by the initial oxide layer [24]. Ermoline [25] reported that the thermal accommodation coefficient is a critical parameter for understanding the heat transfer effects, and nanoparticle ignition is governed mostly by the free molecular heat transfer mechanism. For the scope of application of these mechanisms, the difference mainly considered in previous studies is that, in most cases, the diffusion oxidation mechanism is suitable for large micron-sized particles at a low heating rate, while the melt dispersion mechanism is suitable for small particles (nanometer level) at a high heating rate. In the cases of this study, from the perspective of experimental phenomena, individual aluminum particles below 10 μm followed the melt dispersion mechanism at a heating rate of ~10^6 W/cm^2.

Figure 10 shows some representative snapshots of the laser-induced ignition and combustion of another individual aluminum particle. The whole process can be found in Supplementary Materials, Video S2. The initial diameter was 10.4 μm; the ignition power density was 9.49 × 10^5 W/cm^2. After being heated by the laser, the individual aluminum particle was ignited at 0.273 ms (Figure 10b). The flame appeared as a weak yellow at 1.909 ms, and there was a bright yellow flame at the lower left corner of the particle (Figure 10c). This showed quasi-steady-state combustion [19]. At 2.546 ms, the aluminum particle was completely covered by a yellow flame owing to a heterogeneous oxidation reaction at the surface. The molten aluminum core was gradually exposed to the oxidant, resulting in steady state combustion (Figure 10d). At 3.091 ms, the aluminum particle burned with a stronger radiation flame (Figure 10e). At 3.818 ms, the combustion peaked, the flame envelope was the largest and the brightness reached its highest (Figure 10f). According to the flame envelope shown in Figure 10c–f, the flame propagation rate reached 20.524 mm/s. After the combustion reached its peak, the flame front gradually shrank (Figure 10g,h) and the flame shrinkage rate was 10.556 mm/s. At 5.0 ms, the combustion extinguished.

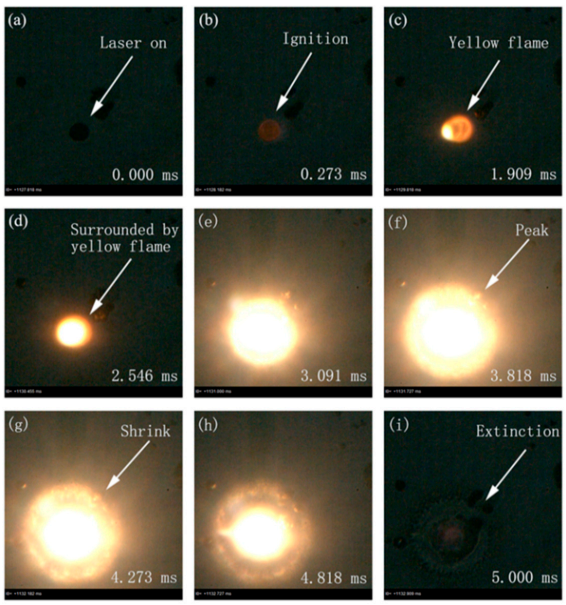

Figure 10. Representative snapshots of laser-induced ignition and combustion processes of an individual aluminum particle. The diameter was 10.4 μm. The laser power density was 9.49 × 10^5 W/cm^2. (Images acquired from Supplementary Materials, Video S2; recording frame: 11,000 fps; exposure time: 90.9 μs).

4. Conclusions

This paper experimentally studied laser-induced ignition and combustion of individual aluminum particles. It was shown that the designed experimental apparatus can provide direct observation for investigating the ignition and combustion behaviors of individual aluminum particles below 10 μm with high spatial and temporal resolutions, by combining laser ignition and microscopic high-speed cinematography. Direct observation shows that, on heating, the diameter and circularity evolution of an individual aluminum particle includes three stages—thermal expansion, melting and evaporation. As the laser power density increases, the duration of each stage shortens. Moreover, the thermal expansion and ignition of individual aluminum particles are heterogeneous.

By upgrading parts of the experimental apparatus, such as the objective and the high-speed camera, higher spatial and temporal resolutions can be reached to meet higher requirements for the investigation of other solid fuels used in rocket propellants.

Supplementary Materials: The following are available online at http://www.mdpi.com/2227-9717/8/3/280/s1: Video S1: Supplementary Materials, Video S1; Video S2: Supplementary Materials, Video S2.

Author Contributions: Conceptualization, X.H. and S.L.; methodology, X.H.; investigation, F.H., S.L., Y.W. and X.H.; data curation, F.H.; writing—original draft, F.H.; writing—review and editing, S.L. and X.H. All authors have read and agreed to the published version of the manuscript.

Funding: This research was funded by the National Natural Science Foundation of China (51976050) and the Natural Science Foundation of Zhejiang Province (LY20E060004).

Conflicts of Interest: The authors declare no conflict of interest.

References

1. Friedman, R.; Maček, A. Combustion studies of single aluminum particles. *Symp. (Int.) Combust.* **1963**, *9*, 703–712. [CrossRef]
2. Friedman, R.; Maček, A. Ignition and combustion of aluminium particles in hot ambient gases. *Combust. Flame* **1962**, *6*, 9–19. [CrossRef]
3. Roberts, T.A.; Rodney, L.B.; Herman, K. Ignition and combustion of aluminum magnesium alloy particles in O_2 at high pressures. *Combust. Flame* **1993**, *92*, 125–143. [CrossRef]
4. Maček, A. Fundamentals of combustion of single aluminum and beryllium particles. *Symp. (Int.) Combust.* **1967**, *11*, 203–217. [CrossRef]
5. Davis, A. Solid propellants: the combustion of particles of metal ingredients. *Combust. Flame* **1963**, *7*, 359–367. [CrossRef]
6. Li, S.; Huang, X.; Zhou, D. Experiments and numerical calculations on laser- induced ignition of single micron-sized aluminum fuel particle. *Propel. Explos. Pyrotech.* **2017**, *42*, 523–531. [CrossRef]
7. Zhu, Y.; Saburo, Y. Effects of oxygen concentration on combustion of aluminum in oxygen/nitrogen mixture streams. *Combust. Flame* **1998**, *115*, 327–334. [CrossRef]
8. Merzhanov, A.G.; Grigorjev, Y.M.; Gal'chenko, Y.A. Aluminium ignition. *Combust. Flame* **1977**, *29*, 1–14. [CrossRef]
9. Bazyn, T.; Herman, K.; Nick, G. Evidence for the transition from the diffusion-limit in aluminum particle combustion. *Proc. Combust. Inst.* **2007**, *31*, 2021–2028. [CrossRef]
10. Benkiewicz, K.; Hayashi, A.K. Aluminum dust ignition behind reflected shock wave: two-dimensional simulations. *Fluid Dyn. Res.* **2002**, *30*, 269–292. [CrossRef]
11. Ohkura, Y.; Rao, P.M.; Zheng, X. Flash ignition of Al nanoparticles: Mechanism and applications. *Combust. Flame* **2011**, *158*, 2544–2548. [CrossRef]
12. Derevyaga, M.E.; Stesik, L.N.; Fedorin, E.A. Ignition and combustion of aluminum and zinc in air. *Combust. Explo. Shock Waves* **1977**, *13*, 722–726. [CrossRef]
13. Legrand, B.; Marion, M.; Chauveau, C.; Gökalp, I. Ignition and combustion of levitated magnesium and aluminum particles in carbon dioxide. *Combust. Sci. Technol.* **2001**, *165*, 151–174. [CrossRef]
14. Widener, J.; Liang, Y.; Beckstead, M. Aluminum combustion modeling in solid propellant environments. In Proceedings of the 35th Joint Propulsion Conference and Exhibit, Los Angeles, CA, USA, 20–24 June 1999.

15. Widener, J.; Beckstead, M. Aluminum combustion modeling in solid propellant combustion products. In Proceedings of the 34th AIAA/ASME/SAE/ASEE Joint Propulsion Conference and Exhibit, Cleveland, OH, USA, 13–15 July 1998.
16. Beckstead, M.W.; Liang, Y.; Pudduppakkam, K.V. Numerical simulation of single aluminum particle combustion. *Combust. Explo. Shock Waves* **2005**, *41*, 622–638. [CrossRef]
17. Liang, Y.; Beckstead, M. Numerical simulation of quasi-steady, single aluminum particle combustion in air. In Proceedings of the 36th AIAA Aerospace Sciences Meeting and Exhibit, Reno, NV, USA, 12–15 January 1998.
18. Koga, K.; Hirasawa, M. Evidence for the anisotropic oxidation of gas-phase Al nanoparticles. *J. Nanopart. Res.* **2015**, *17*, 290.
19. Yang, H.; Yoon, W. Modeling of aluminum particle combustion with emphasis on the oxide effects and variable transport properties. *J. Mech. Sci. Technol.* **2010**, *24*, 909–921. [CrossRef]
20. Ermakov, V.A.; Razdobreev, A.A.; Skorik, A.I.; Pozdeev, V.V.; Smolyakov, S.S. Temperature of aluminum particles at the time of ignition and combustion. *Combust. Explos. Shock Waves* **1982**, *18*, 256–257. [CrossRef]
21. Trunov, M.A.; Schoenitz, M.; Dreizin, E.L. Effect of polymorphic phase transformations in alumina layer on ignition of aluminium particles. *Combust. Theor. Model.* **2006**, *10*, 603–623. [CrossRef]
22. Rai, A.; Park, K.; Zhou, L.; Zachariah, M.R. Understanding the mechanism of aluminium nanoparticle oxidation. Combust. *Theor. Model.* **2006**, *10*, 843–859. [CrossRef]
23. Trunov, M.A.; Schoenitz, M.; Zhu, X.; Dreizin, E.L. Effect of polymorphic phase transformations in Al_2O_3 film on oxidation kinetics of aluminum powders. *Combust. Flame* **2005**, *140*, 310–318. [CrossRef]
24. Levitas, V.I.; Pantoya, M.L.; Dikici, B. Melt dispersion versus diffusive oxidation mechanism for aluminum nanoparticles: Critical experiments and controlling parameters. *Appl. Phys. Lett.* **2008**, *92*, 011921. [CrossRef]
25. Ermoline, A. Thermal theory of aluminum particle ignition in continuum, free-molecular, and transition heat transfer regimes. *J. Appl. Phys.* **2018**, *124*, 054301.